

Ultrasensitive Detection of Interfacial Water Diffusion on Lipid Vesicle Surfaces at Molecular Length Scales

Ravinath Kausik and Songi Han*

Department of Chemistry and Biochemistry and Materials Research Laboratory, University of California, Santa Barbara, California 93106

Received July 28, 2009; E-mail: songi@chem.ucsb.edu

The quantification of interfacial solvent diffusivity on the surface of biomacromolecules is challenging due to the difficulty in distinguishing the surface from bulk solvent signature, the lack of sensitivity in analyzing a population with nearly insignificant quantities compared to bulk water, and the lack of tools to determine its dynamic properties. The interfacial solvent dynamics in the 5–1000 ps regime is a key parameter that is modulated in the hydrophobic collapse occurring in protein folding and aggregation of specific protein segments.^{1,2} The fluctuations in the hydration shell have been shown to strongly couple to and dictate the conformational motion of proteins and, thus, their function.^{3–5} The fluctuations in the hydration shell have been shown to strongly couple to and dictate the conformational motion of proteins and, thus, their function.⁶ The dehydration or hydration effects on lipid surfaces have been proposed to explain membrane fusion, the prominent effects of poly(ethyleneglycol) on membrane (de)stabilization, and protein recognition.^{7–9} Thus, the capability to measure the interfacial diffusion coefficient at specific molecular sites and to characterize the activation energies of solvent diffusion in the hydration shell of biomacromolecules is of fundamental and wide-ranging interest.^{8,9}

In this communication we present measurements of the solvent diffusivity and its activation energy in the hydration shell of unilamellar lipid vesicles dispersed in bulk water. This was made possible by using a recently developed technique of site-specific Overhauser dynamic nuclear polarization (DNP) of the ¹H NMR signal of water at 0.35 T.¹⁰ This technique selectively hyperpolarizes solvent molecules within <5–10 Å of nitroxide radical-based spin labels, providing us with both unique contrast and greatly enhanced sensitivity. Here, we demonstrate unprecedented sensitivity with experiments that are carried out with submicroliter to microliter sample volumes and very low spin label concentrations (<2 mol %). This highlights the feasibility of investigating *real life* samples, such as cellular aggregates, tissue cultures, or rare proteins. It is also important to note that Overhauser DNP acts as a band-selective filter for subnanosecond solvent dynamics at the 0.35 T field employed in our experiments. The complementary technique of field cycling relaxometry (FCR) is sensitive to a wider time scale, including both the much slower nanoseconds dynamics of bound water and the subnanosecond dynamics of the surface hydration water relevant here.^{11,12} An important distinction is also that the Overhauser DNP method only requires ~1/1000 of the sample quantities compared to FCR measurements that are typically carried out on 300–500 μL sample volumes and 5 mol % spin label concentrations. The time required for a complete DNP experiment is ~1 h (including *T*₁ and *T*₁₀ measurements), while FCR experiments typically takes a few hours depending on the number of fields at which the relaxation times are measured. No technique other than the Overhauser DNP approach can measure

the local hydration dynamics at the surface or interface of macromolecules or their assemblies of such minute quantities, in dilute concentrations and under physiologically relevant conditions.

Overhauser DNP relies on the transfer of polarization from the electron spin of nitroxide free radicals to the ¹H of water via dipolar relaxation. The ¹H NMR signal enhancement is given by¹³

$$E_{\max} = 1 - \rho f s_{\max} \frac{|\gamma_S|}{\gamma_I} \quad (1)$$

where E_{\max} is the maximum DNP enhanced ¹H NMR signal, ρ is the coupling factor between the electron and proton, f is the leakage factor describing proton *T*₁ relaxation due to interactions with the electron over all other proton relaxation mechanisms, s_{\max} is the maximum electron spin saturation factor, and γ_S and γ_I are the gyromagnetic ratios of the electron and proton spins. The electron–proton coupling factor is defined by $\rho = (\omega_2 - \omega_0)/(\omega_2 + \omega_0 + 2 \cdot \omega_1 + \omega_1^0)$, where ω_2 , ω_0 , and ω_1 are relaxation rates driven by electron–proton dipolar relaxation and ω_1^0 is the proton relaxation rate in the absence of electron spins. Here, ω_2 is the double quantum dipolar relaxation rate, ω_0 the zero quantum dipolar relaxation rate, and ω_1 the proton single quantum relaxation rate. In essence, ρ carries the information on the proton-bearing molecule's diffusive dynamics with respect to the electron spin label and is, thus, the key parameter to be determined. By measuring the spin–lattice relaxation rates in the presence ($\omega_2 + \omega_0 + 2 \cdot \omega_1 + \omega_1^0$) and absence (ω_1^0) of the spin labels, the leakage factor can be determined following $f = (\omega_2 + \omega_0 + 2 \cdot \omega_1)/(\omega_2 + \omega_0 + 2 \cdot \omega_1 + \omega_1^0)$. The leakage factor, unlike the coupling and saturation factor, critically depends on the spin label concentrations. Thus, by quantifying the leakage factor in conjunction with E_{\max} measurements, differences in spin label concentrations between different samples can be quantitatively accounted for, and thus the coupling factor obtained for different samples. An important characteristic to take into account when employing nitroxide based spin labels is the presence of three ESR lines due to the hyperfine coupling of the electron spin to the ¹⁴N nuclei of the nitroxide radical. To experimentally quantify the saturation factor, full saturation of all ESR transitions, and thus complete exchange of the hyperfine lines, has to be achieved. For spin labels freely dissolved in solutions, the saturation factor can be determined by considering Heisenberg exchange between the colliding electron spins as a function of the spin label concentration.¹⁴ Measuring the DNP enhancements as a function of concentration, and then extrapolating to infinite concentrations, enables us to approach the maximum saturation factor of 1. Thus, the coupling factor can be determined by measuring E_{\max} of eq 1 as a function of spin label concentration and extrapolating to infinite concentrations.¹⁴ Tethered spin labels on macromolecules or assemblies are subject to slowed rotational

tumbling. The resulting decrease in the T_{1n} of ^{14}N nuclei of nitroxides¹⁵ again leads to an efficient mixing between the three nitroxide hyperfine energy levels and therefore enables the possibility of their complete saturation.¹⁴ Thus, even in the absence of Heisenberg spin exchange at the very low spin label concentrations used, the saturation factor can approach 1 at extrapolated high power.¹⁴ In such cases, the analysis does not require measurements of DNP enhancements at a series of concentrations in order to approach the limit of saturation factor of 1. We experimentally tested the validity of this assumption on our lipid vesicle systems by comparing enhancements measured with varying degrees of spin label concentrations (1–10 mol %) distributed on lipid headgroups, whereby the degree of electron spin label dipolar coupling, and thus the ESR line width, is varied. Our finding that the coupling factor remains constant as a function of spin label concentration provides strong evidence that all hyperfine states in these sample systems are well mixed.

The fluctuations in the proton–electron dipolar interaction due to the solvent dynamics can be described in terms of a single correlation time that lies in the tens of picoseconds to subnanosecond time scale, and this enables the use of a single spectral density function to describe the interaction. Thus, once the coupling factor is determined, the translational correlation time of the interacting species can be obtained using the appropriate spectral density function. We use the force free hard sphere dynamic model for the spectral density function, which has been shown to adequately describe the surface relaxation in spin labeled soft matter systems whose interfacial hydration dynamics is dominated by translational diffusion.¹⁶ Although variations of this model including the effects of off-center rotational contributions of spin labels and spin labeled molecules exist,^{15,16} they have been shown to provide similar fit parameters.¹⁰ The translational correlation times obtained from the spectral density function are related to the diffusion coefficients by

$$\tau = \frac{d^2}{D_I + D_S} \quad (2)$$

where D_I and D_S are the diffusion coefficients of the proton and electron spin-bearing molecules, and d is their distance of closest approach. For systems where d is known, one can express the total diffusivity in terms of solvent diffusivity D_I alone in the limit $D_I \gg D_S$, which is valid for tethered spin labels. However, if both d and D_I are variables, we express the solvent dynamics in terms of τ , the translational correlation time of the solvent with respect to the spin label. For spin labels freely dissolved in solution, the diffusion coefficients D_S and D_I were accurately determined by pulsed field gradient NMR measurements, yielding a distance of closest approach of 4.5 Å from eq 2. Using this value for spin labels freely dissolved in bulk water, the diffusion coefficients were determined by DNP as a function of temperature. Assuming Arrhenius behavior ($D = D_0 \exp(-E_A/RT)$) for the temperature dependence of the diffusion coefficients between 295 and 330 K, we can extract the activation energy, E_A , of the diffusion process. The temperature dependence of these dynamic processes, and thus E_A , will be unaltered and therefore correct, even if there was a scaling of the absolute values of our experimental diffusion coefficients determined by the Overhauser DNP analysis.

The DNP-measured temperature dependence of bulk water self-diffusion coefficients is plotted as open circles in Figure 1, which show that they reproduce the known activation energy of $E_A = 19.2$ kJ/mol.¹⁹ This presents an important validity check for our analysis. We further measure the diffusion coefficients and activa-

tion energy of the interfacial solvent of lipid vesicle surfaces. The diffusivity of the surface hydration layer on unilamellar DOTAP (1,2-dioleoyl-3-trimethylammonium-propane) and DPPC (1,2-di-

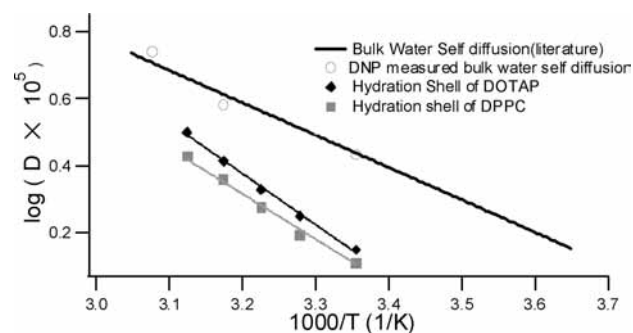


Figure 1. Temperature dependence for bulk water self-diffusion (○) plotted along with literature values¹⁹ for comparison. The temperature dependence for the hydration shell of DOTAP and DPPC vesicle surfaces are also shown.

palmitoyl-*sn*-glycero-3-phosphocholine) vesicles were measured using 1–2 mol % of probe lipid molecules made of 1,2-dioleoyl-*sn*-glycero-3-phospho(tempo)choline lipids spin labeled at the headgroup. We found the translational correlation time (i.e., similar to lifetime) for the interfacial solvent to be $\tau = 165 \pm 16$ ps for DOTAP and $\tau = 185 \pm 18$ ps for DPPC surfaces. Assuming the same 4.5 Å distance of closest approach for hydrated surfaces as that for hydrated molecules, the solvent diffusion coefficient at 295 K is $D = (1.2 \pm 0.10) \times 10^{-9}$ m²/s on DOTAP and $D = (1.1 \pm 0.10) \times 10^{-9}$ m²/s on DPPC lipid vesicle surfaces. These values are about half of the bulk water self-diffusion coefficient of $D = 2.3 \times 10^{-9}$ m²/s and in agreement with the few experimental values reported in literature, e.g. the solvent diffusion on lipid vesicle or peptide surfaces as measured by quasi elastic neutron scattering or FCR analysis.^{8,12,20} Also, the determined translational correlation times of the interfacial solvent are in agreement with values previously discussed in the literature.^{23,24}

Table 1. Surface Diffusivities Determined by Overhauser DNP Analysis^a

samples	τ (ps)	D [10^{-9} m ² /s]	surface charge
poly(aspartic acid) ²¹	192(19)	1.1(0.15)	negative
DOPG/DOPC vesicle	213(21)	0.9(0.10)	
DPPC vesicle	185(18)	1.1(0.10)	zwitterionic
DOTAP vesicle	165(16)	1.2(0.10)	positive
tau (Δ 187) protein ²²	165(16)	1.2(0.10)	
poly(vinylimidazole) ²¹	126(12)	1.6(0.20)	

^a The uncertainty in the experimental values are given in parentheses.

By further examining the solvent dynamics on various other hydrated surfaces of proteins and polyelectrolytes (Table 1), we found that the translational correlation times on negatively charged surfaces are longer with $\tau \approx 185$ –225 ps ($D \approx (0.9$ – $1.1) \times 10^{-9}$ m²/s @ $d = 4.5$ Å) compared to positively charged surfaces with $\tau \approx 125$ –168 ps ($D \approx (1.2$ – $1.6) \times 10^{-9}$ m²/s @ $d = 4.5$ Å), regardless of the chemical specificity of the surface. This finding is interesting but not necessarily surprising, since the surface geometry and the electrostatic interaction are expected to be key determinants for the translational freedom of hydration water.^{6,23}

While the distance of closest approach on hydrated surfaces should be close to that of hydrated molecules, the electrostatic potential of charged lipid surfaces may slightly alter d , thus affecting the apparent D_I value. In such cases where d may be a variable or

a potentially unknown parameter, we put forth the measurement of the solvent diffusivity as a function of temperature, thus acquiring the activation energy of solvent diffusion as a generally applicable approach.

The activation energies of the interfacial solvent diffusion on the surface of DOTAP and DPPC vesicles were determined between temperatures of 295 and 330 K. Arrhenius behavior has been found and activation energies of $E_A = 31 \pm 3$ kJ/mol for DOTAP ($T_m = 273$ K) and $E_A = 27 \pm 2$ kJ/mol for DPPC ($T_m = 314$ K) have been measured. The elevation of activation energies in the hydration shell compared to bulk ($E_A = 19.2$ kJ/mol) by ~ 10 kJ/mol validates the expectation that water dynamics is perturbed at the lipid surface by surface potentials that hinder the diffusion process. Diffusion coefficients of $\sim 0.66 \times 10^{-9}$ m²/s and activation energies of 22 kJ/mol have been reported on POPC lipid vesicle surfaces by field cycling relaxometry analysis.¹² We also verified that the temperature dependence of the here discussed hydration water's diffusion coefficient at the DPPC surface follows Arrhenius behavior across the gel to liquid crystalline phase transition ($T_m = 314$ K) between 295 and 320 K (Figure 1), unlike the lipid segment mobility that experiences a sharp phase transition. The magnitude of both E_A and D values, together with the absence of a concurrent phase transition with the lipid chains, confirms that we are probing bulk-like, dynamic, and not lipid-bound, hydration water properties.

Finally, we focus on the distinctly different E_A values found for DOTAP versus DPPC lipid headgroups. The higher E_A for DOTAP indicates that the interfacial water experiences a stronger attraction to the positively charged trimethylammonium headgroup of DOTAP compared to the zwitterionic phosphatidylcholine group of DPPC. Note also that a shorter correlation time (τ) was measured for DOTAP compared to DPPC surfaces. This finding together with the larger E_A is plausible with a slightly reduced d for DOTAP that reduces τ proportional to d^2 , so that overall τ is reduced despite concurrently slowed solvent diffusion coefficients on DOTAP surfaces (eq 2). The reduction of d between the lipid headgroup-tethered spin label and the ¹H of surface water may occur because of the attraction of the oxygen of water to the DOTAP surface.

The Overhauser DNP technique makes the systematic analysis of a large parameter space of various lipid systems as well as the study of real life systems feasible, because only minute sample quantities are needed. An important strength of this technique is also the possibility of concurrent electron spin resonance analysis of polarity and chain rotational dynamics of the very same samples *in situ*. Some of the sources of error include sample heating, the use of the force free hard sphere model for the determination of the correlation times and the assumption the maximum saturation factor. To overcome heating effects, air is blown on the sample at a steady rate to keep the temperature constant. The development of a more advanced dynamic model for the spectral density function as well as the quantification of the saturation factor is an ongoing effort of the DNP community,^{25,26} given the importance of knowing the interfacial diffusion coefficient as well as the general lack of experimental approaches to these quantities. While our experiments have been carried out at 0.35 T and are thus sensitive to motions

in the picoseconds to subnanosecond time scale, the technique could be extended to cover other time scales as well by carrying out DNP at different field strengths. Overhauser DNP for example will capture tens of nanoseconds hydration dynamics at 0.04 T or sub-to several picoseconds dynamics at 7 T. DNP at multiple fields is currently being explored in our lab and will be reported elsewhere.

Quantifying the surface hydration dynamics of lipid vesicle systems by means of their activation energy in a lipid-specific fashion by employing specifically spin-labeled lipids presents an unprecedented capability. It has very important and wide-ranging implications for the study of membrane fusion, transport, or stability, as well as for the study of lipid raft formation and dynamics.^{7–9}

Acknowledgment. This work was supported by the MRL program of the National Science Foundation (NSF) under Grant No. DMR05-20415, by the NSF Faculty Early CAREER Award (CHE-0645536) to S.H., and the Packard Fellowship for Science and Engineering awarded to S.H. We thank Brandon Armstrong and John Franck for valuable discussions on the Overhauser theory; Hongjun Liang, Galen Stucky, and Cecilia Leal for their initial help in preparing lipid vesicle samples; and Seyma Ozturk for her assistance in sample preparation as well as measurements.

References

- (1) Chandler, D. *Nature* **2005**, *437*, 640–647.
- (2) Frauenfelder, H.; Fenimore, P. W.; Chen, G.; McMahon, B. H. *Proc. Natl. Acad. Sci. U.S.A.* **2006**, *103*, 15469–15472.
- (3) Frauenfelder, H.; Chen, G.; Berendzen, J.; Fenimore, P. W.; Jansson, H.; McMahon, B. H.; Strope, I. R.; Swenson, J.; Young, R. D. *Proc. Natl. Acad. Sci. U.S.A.* **2009**, *106*, 5129–5134.
- (4) Fenimore, P. W.; Frauenfelder, H.; McMahon, B. H.; Parak, F. G. *Proc. Natl. Acad. Sci. U.S.A.* **2009**, *99*, 16047–16051.
- (5) Wood, K.; Plazanet, M.; Gabel, F.; Kessler, B.; Oesterhelf, D.; Tobias, D. J.; Zaccari, G.; Weik, M. *Proc. Natl. Acad. Sci. U.S.A.* **2007**, *104*, 18049–18054.
- (6) Zhang, L.; Yang, Y.; Kao, Y.-T.; Wang, L.; Zhong, D. *J. Am. Chem. Soc.* **2009**, *131*, 10677–10691.
- (7) Hui, S. W.; Kuhl, T. L.; Guo, Y. Q.; Israelachvili, J. *Colloids Surf. B* **1999**, *14*, 213–222.
- (8) Swenson, J.; Kargl, F.; Berntsen, P.; Svanberg, C. *J. Chem. Phys.* **2008**, *129*, 045101.
- (9) Jurkiewicz, P.; Olzyska, A.; Langner, M. *Langmuir* **2006**, *22*, 8749.
- (10) Armstrong, B. D.; Han, S. *J. Am. Chem. Soc.* **2009**, *131*, 4641–4647.
- (11) Persson, E.; Halle, B. *Proc. Natl. Acad. Sci. U.S.A.* **2008**, *105*, 6266–6271.
- (12) Hodges, M. W.; Cafiso, D. S.; Polnaszek, C. F.; Lester, C. C.; Bryant, R. G. *Biophys. J.* **1997**, *73*, 2575–2579.
- (13) Hausser, K. H.; Stehlik, D. *Adv. Magn. Reson.* **1968**, *3*, 79–139.
- (14) Armstrong, B. D.; Han, S. *J. Chem. Phys.* **2007**, *127*, 104508–10.
- (15) Robinson, B. H.; Haas, D. A.; Mailer, C. *Science* **1994**, *263*, 490–493.
- (16) Hwang, L.-P.; Freed, J. H. *J. Chem. Phys.* **1975**, *63*, 4017–4025.
- (17) Ayant, Y.; Belorizky, E.; Fries, P. H.; Rosset, J. *J. Phys. (Paris)* **1977**, *38*, 325.
- (18) Helm, L. *Prog. NMR Spectrosc.* **2006**, *49*, 45–64.
- (19) Wang, J. H.; Robinson, C. V.; Edelman, I. S. *J. Am. Chem. Soc.* **1953**, *75*, 466–470.
- (20) Russo, D.; Hura, G.; Head-Gordon, T. *Biophys. J.* **2004**, *86*, 1852–1862.
- (21) Kausik, R.; Srivastava, A.; Korevaar, P. A.; Stucky, G.; Waite, J. H.; Han, S. *Macromolecules* **2009**, DOI: 10.1021/ma901137g.
- (22) Pavlova, A.; McCarney, E. R.; Peterson, D. W.; Dahlquist, F. W.; Lew, J.; Han, S. *Phys. Chem. Chem. Phys.* **2009**, *11*, 6833–6839.
- (23) Kim, J.; Lu, W.; Qiu, Wang, L.; Caffrey, M.; Zhong, D. *J. Phys. Chem. B* **2006**, *110*, 21994–22000.
- (24) Gawrisch, K.; Gaede, H.C.; Mihalescu, M.; White, S.H. *Eur. Biophys. J.* **2007**, *36*, 281–291.
- (25) Helm, L. *Prog. NMR Spectrosc.* **2006**, *49*, 45–64.
- (26) Kruk, D.; Kowalewski, J. *J. Chem. Phys.* **2002**, *117*, 1194–1200.

JA9060849